The inhibitory effects of 20(R)-ginsenoside Rg3 on the proliferation, angiogenesis, and collagen synthesis of hypertrophic scar derived fibroblasts *in vitro*

Mengyao Tang [1], Wenbo Wang [1], Liying Cheng [1], Rong Jin [1], Lu Zhang [1], Weiwei Bian [1], Yuguang Zhang [1]*

[1] Department of Plastic and Reconstructive Surgery, Shanghai Ninth People's Hospital Affiliated Shanghai Jiao Tong University School of Medicine, 639 Zhizaoju Road, Shanghai, China

A R T I C L E I N F O	**A B S T R A C T**

Objective(s): Therapeutic effect of many selectable methods applied in clinical practice for treating hypertrophic scar (HS) is not still so satisfactory. Meanwhile, a few medicines may lead to several undesirable complications. The traditional Chinese medicine, *Rg3*, has been reported for multiple antitumor effects previously. We have conducted series of animal experiments and confirmed the inhibitory effect of *Rg3* in HS before. The aim of this study was to further verify the conclusions of previous studies and reveal the specific functional mechanisms of *Rg3*.

Materials and Methods: The HS specimens were obtained from the patients aged from 15 to 36 years without systemic diseases and the primary cultured cells were isolated from the scar tissue and expanded *in vitro*. In every experiment, hypertrophic scar fibroblasts (HSFs) were divided into three groups and respectively cultured in medium with or without different *Rg3* concentrations (50, 100 μg/ml). Cell viability assay, flow cytometry analysis (FCM), quantitative PCR, cell migration assay, immunofluorescence staining, western blot and ELISA were employed.

Results: The outcomes demonstrated that *Rg3* could suppress cell proliferation, vascularization and extracellular matrix (ECM) deposition of HSFs *in vitro* by TGF-β/SMAD and Erk signaling pathways. Significant statistical differences were between control group and *Rg3*-treated groups ($P<0.05$).

Conclusion: This study provides sufficient *in vitro* evidences for *Rg3* as a promising drug in the treatment of human HS.

► *Please cite this article as:*
Tang M, Wang W, Cheng L, Jin R, Zhang L, Bian W, Zhang Y. The inhibitory effects of 20(R)-ginsenoside Rg3 on the proliferation, angiogenesis, and collagen synthesis of hypertrophic scar derived fibroblasts *in vitro*. Iran J Basic Med Sci 2018; 21:309-317. doi: 10.22038/ijbms.2018.19451.5153

Introduction

Hypertrophic scar (HS) is one type of the pathologic scars, which responds to the process of wound healing of dermis after skin trauma or serious burns (1). In addition to keloids, HS is characterized by disordered fibrotic proliferation and excessive accumulation of extracellular matrix (ECM) (2). However, they do not invade beyond the boundaries of the original lesions and constantly recrudesce after surgical operation, which serve as the characteristics of keloids (3).

Although the pathogenesis of HS is still ambiguous and indeterminate, the aberrant inflammation, superabundant ECM amassing, expansive neovascularization, lessened apoptosis and atypical ECM remodeling have been reported as the main features and mechanisms of HS formation process (4). Thus, treatments should be targeted at preventing or inhibiting these probable pathological processes. Nowadays, many selectable methods such as pressure therapy, adhesive gel sheet, corticosteroids, etc. are applied in clinical practice and several new treat-ments such as interferon, calcium channel blocker, etc. have been reported (5, 6). Although these methods have their own superiorities, they can only function in certain specific stages and have no effect in other courses of HS formation. Even if they are combined to deal with HS, the therapeutic effect is not still so satisfactory. In addition, a few medicines may bring the risk of systemic diseases, local erythema, molting, pigmentation, wound ulcers and other undesirable complications (7). Therefore, it urged us to seek novel and better treatment strategies or drugs for HS patients.

The time length of wound closure is one of the important factors affecting the occurrence probability of HS (8). Hence, the ideal drugs or other treatments are better to function in the inflammatory phase, which is the first stage of the wound healing process to shorten the healing time of the lesion. Meanwhile, because of the numerous mechanisms during the whole formation process of HS, the treatments should aim at the multiple steps of the entire course.

Corresponding author: Yuguang Zhang. Department of Plastic and Reconstructive Surgery, Shanghai Ninth People's Hospital Affiliated Shanghai Jiao Tong University School of Medicine, 639 Zhizaoju Road, Shanghai, China. Tel: 86-21-63089562; Email: zhangyg18@126.com

Ginseng has been one of the most commonly used herbal medicines in the Orient. Ginsenosides are a group of glycosylated triterpenes, also known as saponins, which represent the pharmacologically active compounds found in the *Panax* root. *Ginsenoside Rg3* is the most active one among ginseng saponins, which includes two different optical isomers named *20(R)-G. Rg3* and *20(S)-G. Rg3*. There have been reported that *G. Rg3* had vigorous biological activity and wide ranges of clinical and pharmacological effects, especially the *20(R)-G. Rg3* (9). Many studies have demonstrated that *Rg3* can inhibit cell proliferation and decrease the angiogenesis of various kinds of tumors (10).

Our previous studies demonstrated that *Rg3* could restrict the excessive inflammation *in vivo*, but do not delay the wound healing process, indicating that *Rg3* could serve as an early intervention to treat HS (11). The previous published researches mainly focused on animal experiments and the effect of implantable *G. Rg3*-loaded electrospun fibrous membranes on HS *in vivo*. To further verify the conclusions of previous studies and reveal the specific functional mechanisms of *Rg3*, we carry out a series of related molecular and cellular experiments *in vitro*, which may consummate the exploration of treatment on HS by *G. Rg3*.

Materials and Methods

Chemicals

G. Rg3 (98.6% purity, Fusheng Pharmaceutical Ltd. Dalian, China) was dissolved in dimethyl sulfoxide (DMSO) and diluted with DMEM solution containing 10% fetal bovine serum (FBS) (HyClone, South Logan, UT) to form the final concentrations gradient (50, 100 µg/ml), as Kim *et al.* described (12). The final concentrations of DMSO in the culture medium were < 0.1%.

Patients

Eighteen Chinese HS patients were recruited in our research. The HS specimens were obtained from these patients aged from 15 to 36 years without systemic diseases. The selected scars were in the active stage and none of them had undergone any treatment before. All the patients were informed of the purpose and procedure of this research and agreed to provide their scars before operations. The HS tissues were completely removed from the patients' skin of face, neck and abdomen. Prior written informed consent was obtained from all participants and every procedure had received the approval of the Ethic Committee.

Culture of hypertrophic scar fibroblasts

The dermis was cut into 1×1 mm pieces after removing the adipose tissues and epidermis. Then, these pieces were digested in 0.25% collagenase for about three hours. After centrifugation and discarding the supernatant, the remaining precipitate including abundant hypertrophic scar fibroblasts (HSFs) and some small pieces of scar tissues were cultured simultaneously in high glucose DMEM (Gibco BRL, Grand Island, NY) supplemented with 10% FBS, penicillin (100 U ml^{-1}) and streptomycin (100 µg ml^{-1}) (Sigma-Aldrich, St Louis, MO) in the 100 mm diameter dishes. They were put into humidified incubator at 37 °C with 5% CO_2. Culture media were replaced every two days. The HSFs gradually attached the bottom surface of the dish or migrated out of the tiny pieces in 3 to 5 days. The second to forth passage of HSFs were used in this research.

Cell viability assay

The viability of HSFs treated with or without *Rg3* was tested by CCK-8 assay (Cell counting kit-8, Dojindo, Kumamoto, Japan). The HSFs were cultured in serum-free medium for 24 hr for synchronization and then seeded in 96-well plates at a density of 1×10^4 cells/ml. After incubating overnight for 24 hr at 37 °C under 5% CO_2, the medium with different *Rg3* concentrations (50, 100 µg/ml) was added into the wells. Ten microliter CCK-8 was added into each well after one, two, three, four and five days of cultivation, respectively. After 2.5 hr of incubation, 100 µl aliquot of incubated medium was pipetted into another 96-well plate, and the colorimetric absorbance was recorded by a microplate reader (Thermo labsystems, Helsinki, Finland) at 450 nm.

Flow cytometric analysis of annexin V-FITC staining

Flow cytometry method (FCM) was used to detect the rate of apoptosis by the annexin V-FITC kit (Miltenyi Biotec, Teterow, Germany). The fibroblasts were incubated in the 6-well plates with the medium containing different *Rg3* concentrations (50, 100 µg/ml). After incubation for 72 hr, the HSFs in each well were collected by centrifugation and resuspended in 500 µl of binding buffer. Ten microliter of annexin V-FITC was added into the HSFs suspension and the mixture was incubated for 10 min at room temperature in the dark. After that, another 10 µl propidium iodide (PI) was added and performed like annexin V-FITC. Finally, the reaction was prevented with ice-bath. We conducted the quantitative analysis by the flowcytometer (BD Bioscience, San Jose, CA). Over 10,000 cells from each well were counted and the apoptotic percentage was quantitatively analyzed by Cell Quest software (BD Bioscience, San Jose, CA).

RNA isolation and quantitative PCR (Q-PCR)

HSFs suspension was added into 10 cm culture dish with a density of 5×10^4 cells/ml. After 48 hr, the medium was changed for new with or without different *Rg3* concentrations (50, 100 µg/ml) and continued to culture for 72 hr. Afterwards, fibroblasts were harvested and total RNA was extracted by Trizol Reagent (Invitrogen, Carlsbad, CA). cDNA was converted from 2 µg of total RNA with Avian Myeloblastosis Virus (AMV) reverse transcriptase (Promega, Madison, WI) in

Table 1. Primer pairs used in Q-PCR analysis are listed as follows

Gene	Primer sequence (5'-3')	Product size (bp)
Type I Collagen	Forward: GGCGGCCAGGGCTCCGACCC Reverse: AATTCCTGGTCTGGGGCACC	319
Type III Collagen	Forward: TGGTGTTGGAGCCGCTGCCA Reverse: CTCAGCACTAGAATCTGTCC	346
Fibronectin	Forward: GCCACTGGAGTCTTTACCACA Reverse: CCTCGGTGTTGTAAGGTGGA	61
α-SMA	Forward: CATCATGCGTCTGGATCTGG Reverse: GGACAATCTCACGCTCAGCA	107
CTGF	Forward: ACAAGGGCCTCTTCTGTGACTT Reverse: GGTACACCGTACCACCGAAGAT	102
PCNA	Forward: GTGATTCCACCACCATGTTC Reverse: TGAGACGAGTCCATGCTCTG	145
TGF-β1	Forward: GAAGTGGATCCACGAGCCCAAG Reverse: GCTGCACTTGCAGGAGCGCAC	227
TGF-β3	Forward: GGTTTTCCGCTTCAATGTGT Reverse: GCTCGATCCTCTGCTCATTC	119
VEGF	Forward: ACGAAGTGGTGAAGTTCATGGAA Reverse: AAGATGTCCACCAAGGTCTCGAT	73
PAI-1	Forward: TCATCATCAATGACTGGGTGAAGAC Reverse: TTCCACTGGCCGTTGAAGTAGAG	127
SMAD-7	Forward: GTGGCATACTGGGAGGAGAA Reverse: GATGGAGAAACCAGGGAACA	309
MMP2	Forward: CGTCTGTCCCAGGATGACATC Reverse: ATGTCAGGAGAGGCCCCATA	59
MMP9	Forward: TTCCAGTACCGAGAGAAAGCCTAT Reverse: GGTCACGTAGCCCACTTGGT	102
MMP13	Forward: ACTGAGAGGCTCCGAGAAATG Reverse: GAACCCCGCATCTTGGCTT	103
IL-6	Forward: TGTAGCCGCCCCACACA Reverse: GGATGTACCGAATTTGTTTGTCAA	68
MCP-1	Forward: CAAACTGAAGCTCGCACTCTCGCC Reverse: ATTCTTGGGTTGTGGAGTGAGTGTTCA	354
α-TNF	Forward: TCTTCTCGAACCCCGAGTGA Reverse: GGAGCTGCCCCTCAGCTT	70
TIMP-1	Forward: CGCTGACATCCGGTTCGT Reverse: TGTGGAAGTATCCGCAGACACT	59
VEGFR	Forward: GAAGGAGAGGACCTGAAACTGTC Reverse: ACTCTTTCAATAAACAGCGTGCTG	458
PDGF	Forward: AGTGACCACTCGATCCGCTCCT Reverse: TTTGGGGCGTTTTGGCTCGCTG	517
GAPDH	Forward: TCACCATCTTCCAGGAGCG Reverse: CTGCTTCACCACCTTCTTGA	572

α-SMA, alpha-smooth muscle actin; CTGF, connective tissue growth factor; PCNA, proliferating cell nuclear antigen; TGF-β, transforming growth factor-β; VEGF, vascular endothelial growth factor; PAI-1, plasminogen activator inhibitor-1; Smads, drosophila mothers against decapentaplegic protein; MMPs, matrix metalloproteinases; IL-6, interleukin 6; MCP-1, monocyte chemoattractant protein-1; α-TNF, tumor necrosis factor alpha; TIMP-1, tissue inhibitor of metalloproteinase-1; VEGFR, vascular endothelial growth factor receptor; PDGF, platelet derived growth factor

a 20 μl of reaction system (4 μl of 5×buffer, 1 μl of oligo-(dT), 2 μl of dNTP, 0.5 μl of RNase inhibitor, 0.5 μl of AMV reverse transcriptase, 12 μl of RNA and ddH$_2$O). The 20 μl of reaction system was incubated at 30 °C for 10 min, 42 °C for 60 min, 95 °C for 5 min, and 5 °C for 5 min. Q-PCR was operated by the Power SYBRGreen PCR master mix (2×) (Applied Biosystems, Foster City, CA) in a real-time thermal cycler (Stratagene Mx3000PTM Q-PCR System, La Jolla, CA). The amplified products were normalized against the internal reference of GAPDH. The primers for Q-PCR analysis are listed in Table 1.

Fibroblast migration assay

For the scratch wound assay, 2×10^5 HSFs were seeded in each well of 6-well culture plates and incubated until reached almost 100% confluence. Then, a scratch wound was created on cells by a sterile 200 μl pipette tip, which was perpendicular to the bottom of the dish. The cell cultures were changed for serum-free DMEM with or without different *Rg3* concentrations (50, 100 μg/ml). Photographs of each wound were taken in five random views under a microscope (Nikon, Tokyo, Japan) immediately or at assigned time point (24 hr or 48 hr) after scratch. The results were quantified and analyzed by the commercial software Image pro-plus version 6.0 (Media Cybernetics, Silver Spring, MD) and public domain image processing program. Data (mean±SD, n=3) were expressed as the percentage of the scratched cell-free zone filled by HSFs.

For the transwell assay, the transwell chambers with 8 μm membrane pore size were put into 24-well plates. After cultivation overnight in serum-free medium, the cell suspensions (1×10^5 cells/well) were added into the upper chambers and incubated with or without different *Rg3* concentrations (50, 100 μg/ml) for 24 hr and 48 hr. Medium with 10% FBS was put into the lower chamber. After incubation for specific time period, cells remaining on the upper surface of the membrane were completely removed away by a cotton swab. Afterwards, fibroblasts that migrated to the bottom surface of the membrane were fixed with 4 % paraformaldehyde and stained with DAPI dye. The number of migrated cells was counted in five random fields under the fluorescence microscope (Olympus, Tokyo, Japan).

Immunofluorescence staining for type I collagen, α-SMA expression and ki-67

HSFs were seeded in the 6-well plates at a density of 2×10^4 cells/ml. After 2-3 days of regular cultivation, the medium was changed for new, which contained different *Rg3* concentrations (50, 100 μg/ml) and the cultivation was continued for another 72 hr. Afterwards, HSFs were fixed in paraformaldehyde and the cell membranes were permeabilized by Triton X-100. After incubated overnight at 4 °C with primary antibodies against type I collagen, alpha-smooth muscle actin (α-SMA) and ki-67 (rabbit anti-human, Abcam, Cambridge,

MA), the cells were cultivated with appropriate fluorescent secondary antibodies (goat anti-rabbit, Jackson Immunoresearch Laboratories, West Grove, PA). The nuclei were stained with DAPI. The positive cells (green) and nuclear DAPI dye (blue) were photographed under a fluorescence microscope (Olympus, Tokyo, Japan). The staining of each section that represented expression level was compared between different groups. The incorporation ratio of ki-67-positive cells was calculated by dividing the number of ki-67-positive cells to total cells. The outcomes were counted in five randomly selected fields.

Western blot analysis

Western blot analysis was performed essentially as described previously (13), with primary antibodies specific for type I collagen, type III collagen, fibronectin, p-SMAD2, p-SMAD3, total-SMAD2/3, SMAD7, p-Erk1/2, and total-Erk1/2 (Cell Signaling Technology, Beverly, MA). The Western blots were developed using a Super-GL ECL reagent (Novland, Shanghai, China) and exposed onto a KODAK X-Omat BT Film (Kodak, New York). The outcomes were analyzed by digital imaging system equipped with AlphaEaseFC software (Alpha Imager 2000, Alpha Innotech).

ELISA assay

HSFs suspension was added into 6 cm culture dish with a density of 4×10^4 cells/ml. After 48 hr, the culture medium was replaced with serum-free DMEM with or without different *Rg3* concentrations (50, 100 μg/ml) and continued to culture for another 72 hr. Afterwards, the culture media that contained the released transforming growth factor-beta 1 (TGF-β1) and vascular endothelial growth factor (VEGF) proteins from HSFs were collected and measured by ELISA Development Kits (R&D Systems, Minneapolis, MN). The absorbance measurement was implemented at a wavelength of 450 nm by a microreader (Thermo Fisher Scientific, Waltham, MA).

Statistical analysis

All assays were performed in triplicate and repeated in three samples. The data were presented as mean±standard deviation (SD). The differences among groups were measured by one-way ANOVA test and differences between two groups were tested with a *post-hoc* statistical method. SPSS 21.0 software (Chicago, IL) was used in statistical analysis. *P*<0.05 is considered as statistically significance.

Results

Ginsenoside Rg3 inhibited HSFs proliferation and induced apoptosis at high concentration

CCK-8 assay was used to detect the effect of *Rg3* on HSFs proliferation. As shown in Figure 1(a), both of the two *Rg3*-treated groups could obviously inhibit HSFs proliferation after 48 hr of incubation compared
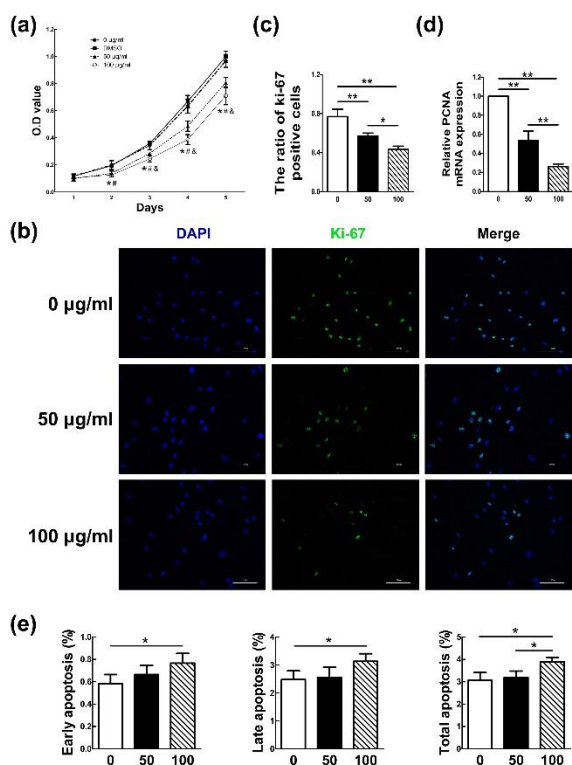
Figure 1. Hypertrophic scar fibroblasts (HSFs) proliferation could be effectively inhibited by *Rg3* and the apoptosis could be induced at high *Rg3* concentration. The proliferation rates in the HSFs treated with or without different *Rg3* concentrations (50, 100 µg/ml) at day 1, 2, 3, 4, and 5 are showed in Figure 1(a). Both of the two *Rg3*-treated groups could obviously inhibit HSFs proliferation after 48 hr of incubation (*$P<0.05$). However, the apparent difference between 50 µg/ml and 100 µg/ml *Rg3*-treated group was detected from day 3 (&$P<0.05$). Apparent difference also existed between DMSO group and *Rg3*-treated groups (#$P<0.05$). As shown in Figure 1(b) and 1(c), the expression of the proliferation marker Ki-67 in *Rg3*-treated groups was clearly decreased as fewer HSFs were able to merge Ki-67 (*$P<0.05$, **$P<0.01$). The level differences of the proliferating cell nuclear antigen (PCNA) proliferation gene between experimental and control groups were showed in Figure 1(d). Evident difference existed between the two groups (**$P<0.01$). The results of flow cytometry analysis in Figure 1(e) showed that obvious difference existed not only between control group and 100 µg/ml-*Rg3*-treated group (**$P<0.01$), but also between the two experimental groups. However, there was no obvious difference between the control group and 50 µg/ml-*Rg3*-treated group in each apoptosis phase

with the control group (*$P<0.05$). However, the apparent difference between 50 µg/ml and 100 µg/ml *Rg3*-treated groups was detected from day 3 (&$P<0.05$). There also was apparent difference between DMSO group and *Rg3*-treated groups (#$P<0.05$), but no obvious difference was found between control group and DMSO group.

Then, the Ki-67 immunofluorescence in combination with DAPI nuclear staining was performed. As shown in Figure 1(b), the expression of the proliferation marker Ki-67 in *Rg3*-treated groups was clearly decreased as fewer HSFs were able to merge Ki-67 compared with that in control group, and the difference of percentages of Ki-67-positive cells

between non-treated and *Rg3*-treated groups was demonstrated in Figure 1(c) (*$P<0.05$, **$P<0.01$).

Meanwhile, the difference of the proliferating cell nuclear antigen (PCNA) proliferation gene between experimental and control groups was detected by Q-PCR. There was significant difference between each two groups (**$P<0.01$) as shown in Figure 1(d). The mRNA expression of PCNA was obviously decreased as the *Rg3* concentration increased.

The results of FCM in Figure 1(e) showed that there only was statistical difference between control group and 100 µg/ml-*Rg3*-treated group in separate early apoptosis phase and late phase (*$P<0.05$). Statistical difference is not only between control group and 100 µg/ml-*Rg3*-treated group (**$P<0.01$), but also there is between the two experimental groups. However, there was no obvious difference between the control group and 50 µg/ml-*Rg3*-treated group in each apoptosis phase.

G. Rg3 reduced collagen production and ECM accumulation

The mRNA or protein levels of collagen I, and III, fibronectin, connective tissue growth factor (CTGF), Interleukin 6 (IL-6), monocyte chemoattractant protein 1 (MCP-1), tumor necrosis factor alpha (α-TNF), α-SMA, TGF-β3, the ratio of *matrix metalloproteinase-2/tissue inhibitor of matrix metalloproteinase 1* (*MMP2/TIMP1*), *MMP9/TIMP1* and *MMP13/TIMP1* quantified in HSFs by Q-PCR and Western blot were showed in Figure 2. Treatment of *Rg3* could visibly suppress both mRNA and protein levels of collagen I, and III and fibronectin as shown in Figure 2(a) and (e). Moreover, *Rg3* apparently reduced the levels of other pro-fibrogenic genes such as CTGF, IL-6, MCP-1, α-TNF, and α-SMA (Figure 2(b)), and simultaneously strengthen the level of anti-fibrosis gene such as TGF-β3 (Figure 2(d)) in HSFs. There is difference between the two groups (*$P<0.05$, **$P<0.01$). Furthermore, the incubation of *Rg3* could distinctly raise the ratio of *MMP2/TIMP1*, *MMP9/TIMP1* and *MMP13/TIMP1*. There were also evident differences between the two groups (*$P<0.05$, **$P<0.01$), which are demonstrated in Figure 2(c).

G. Rg3 restrained cell migration

We applied the scratch wound assay and a transwell system to assess the migration ability of HSFs under the treatment of *Rg3*. As shown in Figure 3(a), the HSFs in control group migrated 50.84±2.78% (mean±SD) of the scratched area, which showed blurry wound boundary after 24 hr of cultivation. The two sides of the wound that almost converged as 87.78±5.14% (mean±SD) of the scratched area were filled after 48 hr of cultivation. In comparison with the control group, the migration ability of HSFs in treated groups was remarkably weakened (*$P<0.05$, **$P<0.01$). The results were further confirmed by a transwell assay. As shown in Figure 3(b), *Rg3* diminished the migration capability of HSFs by reducing cell numbers across the chamber
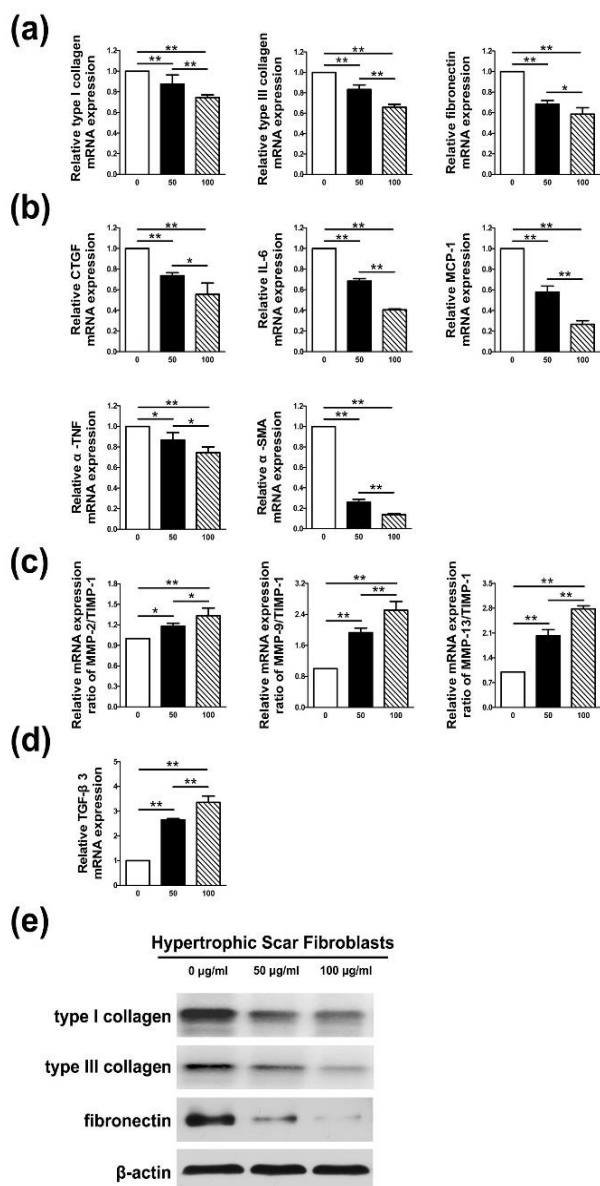
(a)

(b)

(c)

(d)

(e)

Figure 2. Collagen production and extracellular matrix (ECM) accumulation could be reduced by *Rg3*. As shown in Figure 2(a) and (e), *Rg3* could visibly suppress both mRNA and protein levels of collagen I, and III and fibronectin. It could be observed in Figure 2(b) and (d) that *Rg3* apparently reduced the levels of pro-fibrogenic genes such as connective tissue growth factor (CTGF), Interleukin 6 (IL-6), monocyte chemoattractant protein 1 (MCP-1), tumor necrosis factor alpha (α-TNF), and alpha-smooth muscle actin (α-SMA), and simultaneously strengthen the level of anti-fibrosis gene such as transforming growth factor-beta 3 (TGF-β3). The difference existed between the two groups (*$P<0.05$,**$P<0.01$). As shown in Figure 2(c), *Rg3* could distinctly raise the ratio of matrix metalloproteinase-2/tissue inhibitor of matrix metalloproteinase 1 (MMP2/TIMP1), MMP9/TIMP1 and MMP13/TIMP1 (*$P<0.05$, **$P<0.01$), which signified the reduction of fibrotic ECM in hypertrophic scar fibroblasts

membrane in a concentration-dependent manner. There was distinct difference between the two groups at both time points (*$P<0.05$, **$P<0.01$).
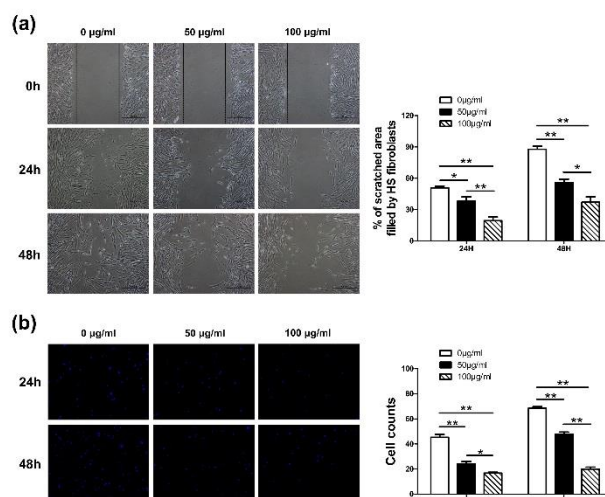

Figure 3. Cell migration was restrained by *Rg3*. As shown in Figure 3(a), the proportion of hypertrophic scar fibroblasts (HSFs)' migrated area in control group was distinctly larger than that in treated groups after both time points. The migration ability of HSFs in treated groups was remarkably weakened (*$P<0.05$, **$P<0.01$). As shown in Figure 3(b), *Rg3* diminished the migration capability of HSFs by reducing cell numbers across the chamber membrane in a concentration-dependent manner (*$P<0.05$, **$P<0.01$)
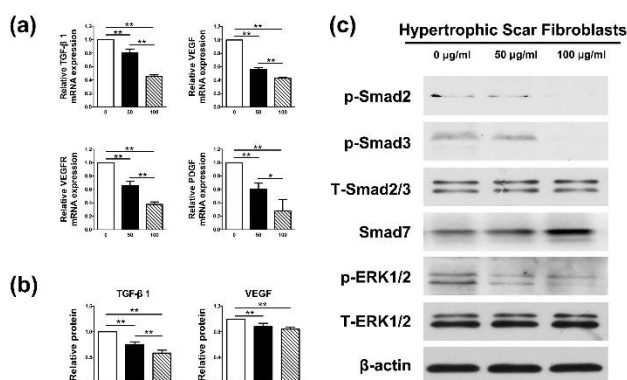

Figure 4. The biological states of hypertrophic scar fibroblasts (HSFs) were changed by *Rg3* via TGF-β/SMAD and Erk signaling pathways. As shown in Figure 4(a) and (b), *Rg3* apparently reduced both mRNA and protein expression levels of transforming growth factor-beta 1 (TGF-β1) and vascular endothelial growth factor (VEGF) as well as the mRNA levels of VEGF receptor (VEGFR) and platelet-derived growth factor (PDGF) (*$P<0.05$, **$P<0.01$). Meanwhile, *Rg3* elevated the protein level of SMAD-7, which served as the negative feedback regulator in TGF-β1/SMAD pathway as shown in Figure 4(c). Furthermore, *Rg3* obviously reduced the protein levels of phosphorylated SMAD2 and phosphorylated SMAD3, which acted as the downstream signal molecules after TGF-β1. The phosphorylated Erk1/2 was also overtly reduced in experimental groups as demonstrated in the results of western blot.

G. Rg3 affected the biological state of HSFs through TGF-β/SMAD and Erk signaling pathways

Several researches have proved that TGF-β1/SMAD and Erk pathways play crucial roles in fibrotic pathogenesis (14). As shown in Figure 4(a) and (b), both

mRNA and protein expression levels of TGF-β1 and VEGF as well as the mRNA levels of VEGF receptor (VEGFR) and platelet-derived growth factor (PDGF) were remarkably decreased by *Rg3*. The statistical differences existed between control group and treated groups (*$P<0.05$, **$P<0.01$). Meanwhile, as demonstrated in Figure 4(c), the protein level of SMAD-7 was distinctly increased in *Rg3*-treated groups. Furthermore, the remedy of *Rg3* obviously reduced the protein levels of phosphorylated SMAD2 and phosphorylated SMAD3. Simultaneously, the phosphorylated Erk1/2 was also overtly reduced in *Rg3*-treated groups in comparison with the control group in HSFs as demonstrated in the results of western blot. The protein levels of total SMAD2/3 and total Erk1/2 remained nearly the same in the three groups.

Discussion

The specialists have been familiar with the common approaches dealing with HS. However, the treatment for HS is still a thorny problem, which is embodied in several aspects as follows: 1) The treatment time is too long. 2) Lack of specific remedies. Various different treatments must join to apply, which are still not so much effective for the scar disease. 3) Many drugs have side-effects, leading to the limit of dosage and cure time. 4) The lack of early interventions may deprive the optimal time for treating. In light of the points listed above, we attempted to seek for a new drug, which may serve as the early intervention to treat HS more effectively or intensify the function of corticosteroids and chemotherapeutic agents.

As a kind of traditional Chinese medicine, *Rg3* has been widely studied in many fields especially in tumor therapy (15). It has been confirmed in our previous researches that Rg3-loaded electrospun fibrous membranes could significantly inhibit HS formation on rabbit ears, with decreased production of collagen fibers and microvessels (11). In the present study, we further probed into the specific functional mechanisms of *Rg3* and carried out related molecular and cellular experiments *in vitro*. The results demonstrated that the proliferation, angiogenesis and collagen synthesis of HSFs could be inhibited by *Rg3* through TGF-β/SMAD and Erk signal pathways.

G. Rg3 has been revealed to decrease various tumor cells proliferation and promote apoptosis (16-18). Li Y *et al.* showed that Rg3 could effectively inhibit cell proliferation and induced apoptosis of multiple myeloma cells (16). In another study, it was reported that *Rg3* both *in vitro* and *in vivo* had anti-proliferative function against melanoma by decreasing histone deacetylase 3 (HDAC3) and increasing acetylation of p53 (17). Other findings demonstrated that *Rg3* could inhibit cell proliferation and promote apoptosis by increasing mitochondrial reactive oxygen species in human leukemia Jurkat cells (18). In our study, it

could be confirmed that *Rg3* has anti-proliferative function in HSFs. The cell proliferation assay, immuno-fluorescence (Ki-67) and decreased expression of PCNA in experimental groups indicated that *Rg3* could suppress the growth of HS effactually. Meanwhile, the FCM outcome showed that only the high concentration of *Rg3* could induce cell apoptosis.

As stated before, the excess collagen deposition and aberrant accumulation of ECM are the main features of HS. The levels of collagen I, collagen III, elastin, fibronectin, etc. all visibly elevate in HS and they function crucially in the formation of fibrotic ECM environments and matrix network (19). In our work, *Rg3* treatment down-regulate both mRNA and protein levels of collagen I, collagen III and fibronectin. Numerous pro-fibrogenic molecules such as CTGF, IL-6, MCP-1, α-TNF, α-SMA, etc. play important roles in the process of HS formation, and higher levels of them have been found in HS versus normal dermis (20-23). In our study, these pro-fibrogenic molecules were all obviously declined after *Rg3* treatment. Additionally, the balance between MMPs and their corresponding inhibitors TIMPs is pivotal in the normal wound healing process (24). The disproportionality of them could impact on natural wound healing and lead to the formation of pathological scars. It has been reported that MMP-2, MMP-9 and MMP-13 contributed mainly to degrade collagen I and collagen III in HS or keloid (25, 26). In our research, the ratios of *MMP2/TIMP1*, *MMP9/ TIMP1* and *MMP13/TIMP1* were adjusted to signi-ficantly higher levels in *Rg3*-treated groups, which implied the inhibition or reversal of fibrosis in HS after *Rg3* treatment. All the results above indicated that *Rg3* could reduce collagen production and ECM accumulation in HS.

It is accepted that a wide variety of profibrotic and anti-fibrotic cytokines are involved in the normal process of wound healing, keeping dynamic equilibrium with each other (19). Among these cytokines, TGF-β family are the extremely pivotal ones associated with many biologic behaviors such as cell proliferation, migration, ECM remodeling, inducing fibrosis, modulating other signal pathways, etc. (27). Once injury occurred, TGF-β is released in the site of damage and attracts multiple inflammatory cells and fibroblasts to the wound (28). TGF-β family mainly has three highly conserved subtypes in the human body named TGF-β1, TGF-β2 and TGF-β3. The former two isoforms are related to fibration, which can not only stimulate collagen synthesis but also prevent ECM disintegration (29). On the contrary, TGF-β3 mainly acts to reduce fibrosis and scarring. In the process, the TGF-β receptors (TGF-βRs) receive the stimulus from corresponding antigens and, serving as a downstream mediator of TGF-β action, transmit signals via SMAD signal-transduction pathway (30). Finally, the fibrosis-related genes are activated, leading to collagen production and ECM deposition. In the SMAD family, SMAD7 provides negative feedback

to the pathway by preventing the phosphorylation of SMAD2 and SMAD3, which acted as the downstream signal molecules after TGF-β1, thus blocking the actions of TGF-β1 or TGF-β2. In our research, *Rg3* evidently reduced the levels of TGF-β1, phosphorrrylated SMAD2 and phosphorylated SMAD3, yet increased the level of SMAD7, implying favorable inhibiting effect of *Rg3* in the TGF-β/SMAD signal pathway.

Once the injury occurs, abundant nutrition supply and substance metabolism that come from neovascularization are needed to facilitate the renovation of damaged tissues. VEGF and PDGF play pivotal roles during the process. Therefore, the expression levels of VEGF and PDGF in HS are much higher than that in normal skin (31). After the binding reaction between antigen and antibody, VEGF and PDGF can all activate ERK1/2 signaling pathway and finally trigger the transcription of angiogenesis-related genes (32, 33). Numerous studies showed that *Rg3* had the treatment efficacy against tumor angiogenesis. It is reported that *Rg3* has anti-leukemia effect in some degree due to its anti-angiogenic action via inhibiting PI3K/Akt and ERK1/2 signal pathways (34). In addition, it is suggested that *Rg3* targeted hypoxia-induced multiple signal pathways to down-regulate the level of VEGF in tumor cells (35). In our research, the levels of VEGF/VEGFR, PDGF and activated phosphorylated ERK1/2 were all down-regulated in experimental groups, suggesting the reductive vascularization in HS after *Rg3* treatment.

Conclusion

Overall, our research demonstrated that *Rg3* could suppress HSFs proliferation, vascularization and ECM deposition *in vitro*. The related TGF-β/SMAD and ERK1/2 signal pathways were proved to be involved in *Rg3* action mechanisms. All of our studies that included the previous animal experiments offer the evidences that *Rg3* may serve as a promising medicine in the treatment of human HS. The further clinical tests may need to be conducted in the future to roundly verify the *Rg3* treatment effect.

Acknowledgment

Conflict of Interest

The authors declare no financial or commercial conflict of interest.

References

1. Lorden ER, Miller KJ, Ibrahim MM, Bashirov L, Hammett E, Chakraborty S, *et al*. Biostable electrospun microfibrous scaffolds mitigate hypertrophic scar contraction in an immune-competent murine model. Acta Biomater 2016; 32: 100-109.
2. Guadanhim LR, Gonçalves RG, Bagatin E. Observational retrospective study evaluating the effects of oral isotretinoin in keloids and hypertrophic scars. Int J Dermatol 2016; 55: 1255-1258.
3. Ud-Din S, Bayat A. New insights on keloids, hypertrophic scars, and striae. Dermatol Clin 2014; 32: 193-209.
4. Van der Veer WM, Bloemen MC, Ulrich MM, Molema G, van Zuijlen PP, Middelkoop E, *et al*. Potential cellular and molecular causes of hypertrophic scar formation. Burns 2009; 35: 15-29.
5. Hayashi T, Furukawa H, Oyama A, Funayama E, Saito A, Murao N, *et al*. A new uniform protocol of combined corticosteroid injections and ointment application reduces recurrence rates after surgical keloid/hypertrophic scar excision. Dermatol Surg 2012; 38: 893-897.
6. Yang SY, Yang JY, Hsiao YC. Comparison of combination therapy (steroid, calcium channel blocker, and interferon) with steroid monotherapy for treating human hypertrophic scars in an animal model. Ann Plast Surg 2015; 74 Suppl 2: S162-167.
7. Wang J, Jiao H, Stewart TL, Shankowsky HA, Scott PG, Tredget EE. Improvement in postburn hypertrophic scar after treatment with IFN-alpha2b is associated with decreased fibrocytes. J Interferon Cytokine Res 2007; 27: 921-930.
8. Berman B, Flores F. The treatment of hypertrophic scars and keloids. Eur J Dermatol 1998; 8: 591-595.
9. He B, Chen P, Xie Y, Li S, Zhang X, Yang R, *et al*. 20(R)-Ginsenoside Rg3 protects SH-SY5Y cells against apoptosis induced by oxygen and glucose deprivation/reperfusion. Bioorg Med Chem Lett 2017; 27: 3867-3871.
10. Keung MH, Chan LS, Kwok HH, Wong RN, Yue PY. Role of microRNA-520h in 20(R)-ginsenoside-Rg3-mediated angiosuppression. J Ginseng Res 2016; 40: 151-159.
11. Cheng L, Sun X, Hu C, Jin R, Sun B, Shi Y, *et al*. *In vivo* early intervention and the therapeutic effects of 20(S)-ginsenoside Rg3 on hypertrophic scar formation. PLoS One 2014; 9: e113640.
12. Kim SM, Lee SY, Cho JS, Son SM, Choi SS, Yun YP, *et al*. Combination of ginsenoside Rg3 with docetaxel enhances the susceptibility of prostate cancer cells via inhibition of NF-Kb. Eur J Pharmacol 2010; 10: 1-9.
13. Shin JU, Lee WJ, Tran TN, Jung I, Lee JH. Hsp70 knockdown by siRNA decreased collagen production in keloid fibroblasts. Yonsei Med J 2015; 56: 1619-1626.
14. Chen QJ, Zhang MZ, Wang LX. Gensenoside Rg3 inhibits hypoxia-induced VEGF expression in human cancer cells. Cell Physiol Biochem 2010; 26: 849-858.
15. Shin YM, Jung HJ, Choi WY, Lim CJ. Antioxidative, anti-inflammatory, and matrix metalloproteinase inhibitory activities of 20(S)-ginsenoside Rg3 in cultured mammalian cell lines. Mol Biol Rep 2013; 40: 269-279.
16. Li Y, Yang T, Li J, Hao HL, Wang SY, Yang J, *et al*. Inhibition of multiple myeloma cell proliferation by ginsenoside Rg3 via reduction in the secretion of IGF-1. Mol Med Rep 2016; 14: 2222-2230.
17. Shan X, Fu YS, Aziz F, Wang XQ, Yan Q, Liu JW. Ginsenoside Rg3 inhibits melanoma cell proliferation through down-regulation of histone deacetylase 3 (HDAC3) and increase of p53 acetylation. PLoS One 2014; 9: e115401.
18. Xia T, Wang YN, Zhou CX, Wu LM, Liu Y, Zeng QH, *et al*.

Ginsenoside Rh2 and Rg3 inhibit cell proliferation and induce apoptosis by increasing mitochondrial reactive oxygen species in human leukemia Jurkat cells. Mol Med Rep 2017; 15: 3591-3598.

19. Berman B, Maderal A, Raphael B. Keloids and Hypertrophic Scars: pathophysiology, classification, and treatment. Dermatol Surg 2017; 43 Suppl 1:S3-S18.

20. Ehrlich HP, Desmoulière A, Diegelmann RF, Cohen IK, Compton CC, Garner WL, *et al*. Morphological and immunochemical differences between keloid and hypertrophic scar. Am J Pathol 1994; 145:105-113.

21. Mu S, Kang B, Zenfresultg W, Sun Y, Yang F. MicroRNA-143-3p inhibits hyperplastic scar formation by targeting connective tissue growth factor CTGF/CCN2 via the Akt/mTOR pathway. Mol Cell Biochem 2016; 416: 99-108.

22. Yamamoto T, Hartmann K, Eckes B, Krieg T. Role of stem cell factor and monocyte chemoattractant protein-1 in the interaction between fibroblasts and mast cells in fibrosis. J Dermatol Sci 2001; 26: 106-111.

23. Salgado RM, Alcántara L, Mendoza-Rodríguez CA, Cerbón M, Hidalgo-González C, Mercadillo P, *et al*. Post-burn hypertrophic scars are characterized by high levels of IL-1β mRNA and protein and TNF-α type I receptors. Burns 2012; 38: 668-676.

24. Visse R, Nagase H. Matrix metalloproteinases and tissue inhibitors of metalloproteinases: structure, function, and biochemistry. Circ Res 2003; 92: 827-839.

25. Uchida G, Yoshimura K, Kitano Y, Okazaki M, Harii K. Tretinoin reverses upregulation of matrix metalloproteinase-13 in human keloid-derived fibroblasts. Exp Dermatol 2003; 12 Suppl 2: 35-42.

26. Huang D, Liu Y, Huang Y, Xie Y, Shen K, Zhang D, *et al*. Mechanical compression upregulates MMP9 through SMAD3 but not SMAD2 modulation in hypertrophic scar

fibroblasts. Connect Tissue Res 2014; 55: 391-396.

27. Cheng F, Shen Y, Mohanasundaram P, Lindström M3, Ivaska J4, Ny T, *et al*. Vimentin coordinates fibroblast proliferation and keratinocyte differentiation in wound healing via TGF-β-Slug signaling. Proc Natl Acad Sci U S A 2016; 113: E4320-7.

28. Bullard KM, Longaker MT, Lorenz HP. Fetal wound healing: current biology. World J Surg 2003; 27: 54-61.

29. Kose O, Waseem A. Keloids and hypertrophic scars: are they two different sides of the same coin? Dermatol Surg 2003; 34: 336-346.

30. Branton MH, Kopp JB. TGF-β and fibrosis. Microbes Infect 1999; 1: 1349-1365.

31. Chun Q, ZhiYong W, Fei S, XiQiao W. Dynamic biological changes in fibroblasts during hypertrophic scar formation and regression. Int Wound J 2016; 13:257-262.

32. Wu Y, Zhang Q, Ann DK, Akhondzadeh A, Duong HS, Messadi DV, *et al*. Increased vascular endothelial growth factor may account for elevated level of plasminogen activator inhibitor-1 via activating ERK1/2 in keloid fibroblasts. Am J Physiol Cell Physiol 2004; 286: C905-912.

33. Li J, Zhang M, Ma J. Myricitrin inhibits PDGF-BB-stimulated vascular smooth muscle cell proliferation and migration through suppressing PDGFRβ/Akt/Erk signaling. Int J Clin Exp Med 2015; 8: 21715-21723.

34. Zeng D, Wang J, Kong P, Chang C, Li J, Li J. Ginsenoside Rg3 inhibits HIF-1α and VEGF expression in patient with acute leukemia via inhibiting the activation of PI3K/Akt and ERK1/2 pathways. Int J Clin Exp Pathol 2014; 7:2172-2178.

35. Chen QJ, Zhang MZ, Wang LX. Gensenoside Rg3 inhibits hypoxia-induced VEGF expression in human cancer cells. Cell Physiol Biochem 2010; 26: 849-858.